Comparative Biochemistry and Physiology, Part B 243–244 (2020) 110438

Contents lists available at ScienceDirect

Comparative Biochemistry and Physiology, Part B

journal homepage: www.elsevier.com/locate/cbpb

Single and combined effects of the "Deadly trio" hypoxia, hypercapnia and warming on the cellular metabolism of the great scallop *Pecten maximus*

Sandra Götze[a,*], Christian Bock[a], Charlotte Eymann[a], Gisela Lannig[a], Jennifer B.M. Steffen[b], Hans-O. Pörtner[a,c]

[a] Alfred Wegener Institute Helmholtz Centre for Polar and Marine Research. Am Handelshafen 12, 27515 Bremerhaven, Germany
[b] Marine Biology, Faculty of Mathematics and Natural Sciences, University of Rostock, Rostock, Germany
[c] Fachbereich 2 Biologie / Chemie, Universität Bremen, Leobener Straße, 28359 Bremen, Germany

ARTICLE INFO

Keywords:
^{1}H NMR
Metabolomics
Metabolic pathways
Palaeo-physiology
Ocean climate change

ABSTRACT

In the ocean the main climate drivers affecting marine organisms are warming, hypercapnia, and hypoxia. We investigated the acute effects of warming (W), warming *plus* hypercapnia (WHc, ~1800 µatm CO_2), warming *plus* hypoxia (WHo, ~12.1 kPa O_2), and a combined exposure of all three drivers (Deadly Trio, DT) on king scallops (*Pecten maximus*). All exposures started at 14 °C and temperature was increased by 2 °C once every 48 h until the lethal temperature was reached (28 °C). Gill samples were taken at 14 °C, 18 °C, 22 °C, and 26 °C and analyzed for their metabolic response by ^{1}H-nuclear magnetic resonance (NMR) spectroscopy. Scallops were most tolerant to WHc and most susceptible to oxygen reduction (WHo and DT). In particular under DT, scallops' mitochondrial energy metabolism was affected. Changes became apparent at 22 °C and 26 °C involving significant accumulation of glycogenic amino acids (e.g. glycine and valine) and anaerobic end-products (e.g. acetic acid and succinate). In line with these observations the LT_{50} was lower under the exposure to DT (22.5 °C) than to W alone (~ 25 °C) indicating a narrowing of the thermal niche due to an imbalance between oxygen demand and supply.

1. Introduction

The evolution of marine flora and fauna during Earth's history was shaped more than once by environmental disturbances. Some of the most severe environmental changes led to marine mass extinctions that were triggered by volcanism. The accompanying release of greenhouse gases led, among others, to warming, ocean acidification, changes in ocean currents and stratification, and the consecutive development of anoxic zones (Aberhan and Baumiller, 2003; Bachan and Payne, 2015). The Permian-Triassic (PT) transition was one of the most severe marine crises erasing up to 95% of marine taxa, likely caused by outgassing of Siberian traps (Bambach et al., 2004; Song et al., 2013). Modelled climate changes obtained from stable isotopes suggest a rise in sea surface temperatures by about 11 °C, paralleled by a drop in seawater pH of up to 0.7 pH units due to the subsequent CO_2 uptake by the ocean (Joachimski et al., 2012; Sun et al., 2012; Clarkson et al., 2015). Together with warming the slowdown of the meridional circulation contributed to stratification and depletion of ~76% of global marine oxygen (~ 140 mmol O_2/m^3) causing seafloor anoxia < 5 mmol O_2/ m^3 (Lau et al., 2016; Penn et al., 2018). Today's anthropogenic climate forcing is estimated to be analogous to past crises (Penn et al., 2018) affecting the oceans by the same drivers as in the past, although present changes have not reached past extremes. Current models predict an increase in ocean surface temperature by 1.8–4 °C by the end of the 21th century, and a drop in seawater (SW) pH of 0.3–0.4 pH units (equals ~1000 µatm CO_2) under the most extreme climate scenario (RCP 8.5, see IPCC, 2019). Oxygen solubility decreases with increasing temperature. In stratified water layers or eutrophied, warming coastal waters, oxygen may become fully depleted (Diaz and Rosenberg, 2008; Keeling et al., 2010; Breitburg et al., 2018). Accordingly, the patterns of mass extinctions and impacts on palaeo species may harbour valuable knowledge for understanding the impacts of progressive extant climate change on marine biota when extrapolated into the future. Projected impacts on marine fauna are diverse depending on the type of driver, it's magnitude, duration of exposure, geographical location, species, life stage, and ecosystem interactions (Guinotte and Fabry, 2008; Pörtner,

Abbrevations: ^{1}H NMR, proton nuclear magnetic resonance; W, warming exposure; WHo, warming *plus* hypoxia; WHc, warming *plus* hypercapnia; DT, deadly trio; ANOVA, analysis of variance; PLS-DA, partial least square-discriminant analysis; PCA, principal component analysis; PT, Permian-Triassic; PTME, Permian-Triassic mass extinction; Ma, Million years ago; BCAA, branched chain amino acids; OCLTT, oxygen and capacity limited thermal tolerance; SMR, standard metabolic rate

* Corresponding author at: Alfred Wegener Institute Helmholtz Centre for Polar and Marine Research, Am Handelshafen 12, 27515 Bremerhaven, Germany
E-mail address: Sandra.Goetze@awi.de (S. Götze).

https://doi.org/10.1016/j.cbpb.2020.110438
Received 8 November 2019; Received in revised form 20 February 2020; Accepted 31 March 2020
Available online 03 April 2020
1096-4959/

2012; Wittmann and Pörtner, 2013; Parker et al., 2013).

Assuming that the mechanisms that have shaped the fate of fauna in the deep past are still in place in extant fauna, observed fossil patterns are likely related to the capacity of organisms to tolerate environmental changes. For insights into paleophysiology, bivalve mollusks appear to be ideal model organisms as they are well preserved due to their calcareous shell, and their fossil record covers more than 500 Ma of Earth history. Furthermore, this group did not change drastically in morphology, life style, or presumably physiology, allowing a comparison between palaeo-, and extant forms. Fossil records from the Permian-Triassic mass extinction (PTME) indicate that orders of ostreoida, trigoniida and mytilida performed better than pectinida, myalinida, and pholadomyida and that the latter ones had a higher rate of extinction (Tu et al., 2016). Subtidal pectinids have been shown to be more sensitive to hypoxia or anoxia compared to other bivalves such as ostreoids or mytilids that, as inhabitants of the intertidal, are well adapted to low oxygen concentrations (Shumway and Koehn, 1982; Laing, 2000; Artigaud et al., 2014; Laudien et al., 2002). Furthermore, the anatomy of pectinids differs from other bivalves as they cannot fully close their valves and are able to escape from predators by rapid valve clapping (Wilkens, 2006; Tremblay and Guderley, 2013). Valve clapping requires supplementary energy supply via anaerobic mechanisms, and is associated with accelerated heart rate, stroke volume and depletion of oxygen from the hemolymph (Thompson et al., 1980). Recovery from muscular fatigue relies on an oxygenated environment (Grieshaber, 1978; Bock et al., 2019). Accordingly, we hypothesize that scallops such as *P. maximus* are more vulnerable to environmental changes compared to other bivalves such as oysters.

Temperature extremes, hypercapnia or hypoxia affect marine organisms through functional impairments at various levels with consequences for organismic performance (e.g. reviewed by Kassahn et al., 2009). Full understanding of such impacts requires not only the study of the effects of individual but also of combined drivers. Available results obtained in marine invertebrates and fish imply disturbances in acid-base homeostasis, respiration rates, and stress response pathways with fundamental effects on growth, reproduction and fitness (e.g. Pörtner et al., 2004; Artigaud et al., 2015a, 2015b; Ern et al., 2017; Stapp et al., 2017, 2018). One main underpinning principle shaping tolerance to environmental changes are disturbances in energy homeostasis, when aerobic energy supply becomes constrained, not or not fully meeting the animal's requirements (for more detail see Pörtner, 2002; Guderley and Pörtner, 2010; Sokolova et al., 2012; Pörtner et al., 2017). Under environmental extremes such as oxygen deficiency or heat exposure a systemic disruption of oxygen metabolism (often characterized by the onset of anaerobiosis), and consequently cellular damages and disturbance of homeostasis may occur (Heise et al., 2003, 2006). Intermediate or end-products of cellular pathways characterize such shifts in energetics. Investigations of the metabolome and metabolic pathways provide valuable insights into underlying cellular mechanisms responding to environmental drivers (e.g. Viant et al., 2003; Lenz et al., 2005; Rebelein et al., 2018). Metabolic profiles are species and tissue specific and metabolite biomarkers can be used to assess environmental stress, toxicity and disease (Jones et al., 2008; Ellis et al., 2014; Palma et al., 2019). The accumulation of metabolites involved in anaerobic energy metabolism under environmental drivers such as temperature or ocean acidification, has been shown to be an important indicator of the loss in aerobic scope with strictly time-limited survival (Lannig et al., 2010; Tripp-Valdez et al., 2017; Zittier et al., 2018). The current study is embedded in the larger DFG-funded research unit "Temperature-Related Stresses as a Unifying Principle in Ancient Extinctions" (TERSANE) which combines geochemical studies with paleobiological analyses and physiological experiments focusing on the vulnerability of ostreoids and pectinids under climate change. We selected two representative species from both taxonomic orders, *Ostrea edulis* and *Pecten maximus*, and subjected individuals to acute warming as well as warming under hypoxic and/or hypercapnic conditions, starting at the lower annual habitat temperature until the lethal temperature was reached. To mimick the past the pH was reduced by 0.6 pH units to ~7.5 corresponding to the hypothesized pH reduction during the PTME (Clarkson et al., 2015). In contrast to past oxygen levels that were estimated to be close to anoxia during the PTME (e.g. Wignall and Twitchett, 1996; Weidlich et al. 2003) we chose ~55% air saturation (P_{O2} = 10.7 to 13.5 kPa (3.5 to 5 mg O_2/L) depending on temperature) as we did not want to instantly kill the bivalves but rather investigate mechanisms that are activated in response to oxygen depletion. The present study on the king scallop, *Pecten maximus* focuses on the contribution of various metabolic processes and highlights changes in gill metabolism identified by untargeted metabolic profiling using ^{1}H NMR spectroscopy. We specify potential biomarkers of stress and explain organismic constraints through changes in cellular metabolism under acute warming, combined exposures to warming and hypoxia, warming and hypercapnia, and the combination of all three drivers.

2. Material and methods

2.1. Animal origin and maintenance

In autumn 2017 adult king scallops, *P. maximus*, were caught by scuba divers in the estuary of Vigo at 10 m depth (Spain, ~42°14′46.6"N 8°44′18.5"W). Surface SW temperature was ~18 °C with full salinity. Scallops were transported by car, submerged under aerated water at 10 °C within 24 h to the Alfred Wegener Institute Helmholtz Centre for Polar and Marine Research (AWI, Bremerhaven). Upon arrival, scallops were immediately transferred to the institutional aquarium system filled with North Sea water (14 °C, 32 PSU) and acclimated for at least 4 weeks. Scallops were fed 3 times a week by a mixture of commercial algal blend (Nyos, PhytoMaxx) and a self-cultivated algal mixture including *Rhodomonas spec.*, *Phaeodactylum tricornutum, Chaetocerus spec.*, and *Isochrysis galbana* (minimum 3000 cells/ml SW). Prior to the experiments epibionts were carefully removed (oyster knife, scrubbing) and each scallop was measured, weighed and labelled individually. Afterwards scallops were allowed to recover from handling stress for at least one week. Animals had an average size of 10.4 ± 1.1 cm length, 10.8 ± 1.3 cm width, and weighed 163.4 ± 46.0 g.

2.2. Experimental setup and water chemistry

The experimental setup comprised four exposures running independently: acute warming (W), acute warming *plus* hypercapnia (WHc), acute warming *plus* hypoxia (WHo), and the combination of all three drivers (Deadly trio, DT). All exposures started at 14 °C and temperature was increased by 2 °C every 48 h until 28 °C when the remaining scallops died (T_{Death}). The respective target temperature (± 0.5 °C) was reached within 5 h. Oxygenation and carbon dioxide levels were controlled and mixed by a gas-mixing device (HTK, Hamburg). In W and WHc exposures oxygen levels were kept above 90% air saturation (PO_2 = 19.2 to 20.6 kPa (6.2 to 8.2 mg O_2/L) depending on temperature), and in WHo and DT exposures at ~55% air saturation (PO_2 = 10.7 to 13.5 kPa (3.5 to 5.0 mg O_2/L) depending on temperature). Under WHc and DT PCO_2 levels were set to around 1800 µatm to reach a pH of ~7.5 and under W and WHo to ~550 µatm (pH 8.1). Water parameters were monitored daily as described in Eymann et al. (2020) and the SW physiochemical conditions at each temperature step are shown in Table 1.

P. maximus were randomly assigned to one of the exposures (n = 60 per exposure) and acclimated for a minimum of 3 days. Exposures were carried out in closed-recirculating aquarium systems as described in Eymann et al. (2020). Briefly, each experimental system comprised a header, a receiver (~ 100 l), a reservoir tank (~ 100 l) and four experimental tanks (52 l volume each) which were connected to each other to ensure consistent conditions. Scallops were used partly for

Table 1
Summary of water chemistry parameters during acute warming exposures.

T_{nom} (°C)	T_{meas} (°C)	Sal (PSU)	$pH_{Freescale}$	PO_2 (kPa)	PCO_2 (µatm)
Warming					
14	14.4 ± 0.3	34.4 ± 0.3	8.011 ± 0.037	20.6 ± 0.2	705 ± 87
18	18.2 ± 0.2	34.0 ± 0.5	7.965 ± 0.042	19.4 ± 0.3	712 ± 93
22	22.0 ± 0.1	34.0 ± 0.3	8.035 ± 0.054	19.8 ± 0.8	633 ± 97
26	26.3 ± 0.7	33.3 ± 0.7	7.977 ± 0.035	20.0 ± 0.6	748 ± 66
Warming *plus* hypoxia					
14	14.0 ± 0.1	33.5 ± 0.4	8.103 ± 0.008	12.4 ± 0.6	473 ± 39
18	18.1 ± 0.2	33.8 ± 0.2	8.118 ± 0.006	13.1 ± 0.4	449 ± 8
22	22.0 ± 0.3	34.0 ± 0.2	8.048 ± 0.013	12.5 ± 0.6	538 ± 18
26	26.2 ± 0.1	34.4 ± 0.4	8.011 ± 0.031	13.5 ± 0.5	597 ± 35
Warming *plus* hypercapnia					
14	13.9 ± 0.1	33.5 ± 0.4	7.512 ± 0.021	20.6 ± 0.1	2050 ± 65
18	18.2 ± 0.1	33.8 ± 0.2	7.529 ± 0.009	20.3 ± 0.3	2062 ± 47
22	22.3 ± 0.0	34.0 ± 0.2	7.548 ± 0.012	19.8 ± 0.3	2054 ± 97
26	26.1 ± 0.2	34.4 ± 0.4	7.552 ± 0.018	19.2 ± 0.2	2124 ± 96
Deadly trio					
14	14.4 ± 0.2	33.8 ± 0.9	7.619 ± 0.023	11.7 ± 0.4	1611 ± 78
18	17.8 ± 0.1	34.2 ± 0.4	7.665 ± 0.015	12.0 ± 0.6	1688 ± 280
22	22.2 ± 0.1	34.1 ± 0.2	7.583 ± 0.015	11.0 ± 0.6	1969 ± 192
26	26.3 ± 0.2	33.8 ± 0.0	7.538 ± 0.029	10.7 ± 0.9	2312 ± 78

Temperature (T_{nom} = target temperature and T_{meas} = measured temperature in systems; °C), salinity (PSU), $pH_{Freescale}$, PO_2 (kPa) and PCO_2 (µatm) were determined in water samples collected throughout W, WHo, WHc, and DT exposures. Data are presented as means ± SD (n = 5-7 single measurements).

tissue analysis (n = 26 for W and WHc treatments, respectively (four sampling temperatures); n = 35 for WHo and DT treatments, respectively (four + two additional sampling temperatures to account for the possibility of shifting threshold temperatures, additional data not shown)) and partly to determine the rate of survival. Throughout exposure scallops were fed twice a day to exclude effects of starvation (diet and concentration as indicated earlier) and the aquaria were cleaned regularly of faeces. Levels of nitrite, nitrate and ammonium were monitored and held below critical concentrations by regular SW exchanges (approximately twice a week).

2.3. Survival rate

The survival rate was calculated starting from the number of scallops that were not used for tissue analyses. Thus, calculations based on 34 scallops accounting to 100% in warming and warming *plus* hypercapnia treatments and on 25 scallops in warming *plus* hypoxia and Deadly Trio treatments. Dead scallops were subtracted from the number of residual scallops and the survival rate per temperature step expressed in percent (%). For each exposure the half-maximal lethal temperature (LC_{50}) was determined.

2.4. Tissue sampling

Between six to eight scallops were sacrificed at 14 °C, 18 °C, 22 °C, and 26 °C each, except for WHo when only four scallops survived up to 26 °C, ending the exposure after sampling. Scallops were opened on ice and different tissues (gills, mantle, hepatopancreas, phasic and tonic muscle) were removed quickly, snap-frozen in liquid nitrogen, and stored at −80 °C until further analyses.

2.5. Metabolic profiling

Metabolic profiling was conducted on 5 to 8 gill and phasic muscle samples of each treatment (except for WHo at 26 °C with n = 4) as described in Tripp-Valdez et al. (2017). Briefly, metabolites were extracted from 40 to 50 mg of tissue (fresh weight, FW) by methanol-chloroform extraction. The methanol fraction was dried overnight and the pellet was re-suspended in the 2-fold volume of FW in deuterized water (D_2O) comprising 3-(trimethylsilyl) propionic-2,2,3,3-d4 acid, sodium salt (TSP; 0.05 wt%; Sigma Aldrich, St. Louis, USA) as internal standard. Untargeted metabolic profiling based on one dimensional ^1H NMR spectroscopy was carried out in an ultra-shielded vertical 9.4 T NMR spectrometer (Advance III HD 400 WB, Bruker-BioSpin GmbH, Germany) using a triple tuned ^1H–^{13}C-^{31}P-HRMAS NMR probe. TOPSPIN 3.2 software (TopSpin 3.2, Bruker-BioSpin GmbH, Germany) was used for acquisition and a Call-Purcell-Meiboom-Gill (CPMG) sequence was chosen for metabolic profiling (described in detail in Schmidt et al., 2017). The spectra were baseline, shim, and phase corrected and calibrated to the TSP signal using the software Chenomx NMR suite 8.1 (Chenomx Inc., Canada). Thereafter, metabolites were assigned according to the chemical shift of their NMR signals using the internal database of Chenomx and literature data (e.g. Tikunov et al., 2010, 2014; Capello et al., 2018). Metabolite quantification was based on the integration routine within Chenomx calibrating the TSP signal integral to a concentration of 3.2 mM. Chemical shifts of AMP, ADP, and ATP are difficult to distinguish by the applied method and those signals were summed. The resulting total adenylate concentration (comprising AMP, ADP, and ATP) was not affected by temperature or exposure (p in all cases > 0.124) and was thus used for normalization (see below).

2.6. Statistical analysis

Statistical analysis was carried out with the online platform *Metaboanalyst* (Metaboanalyst 4.0, Xia and Wishart, 2016). Data sets were normalized to the adenylate concentration (sum of AMP + ADP + ATP) and generalized log (g-log) transformed for normal data distribution (Purohit et al., 2004). Unsupervised principle component analysis (PCA) did not detect any outliers. For in depth analysis, temperature and exposure groups were analyzed by one-way ANOVA followed by a post-hoc test (Fisher's LSD; p-value ≤ .05). Significant differences between groups of altered metabolites were displayed as provided by MetaboAnalyst 4.0 using Sigma Plot (12.0, Systat Software, Inc.). Relevant metabolites are presented in the results as millimolar (mM) concentrations normalized to the total adenylate concentration. The distinction of metabolite profiles was identified by a supervised partial least–square discriminant analysis (PSL-DA) analysis. The two components accounting for the highest variance are illustrated as 2D score and the distance of the samples reflect the dissimilarity in metabolite patterns.

2.7. Pathway analysis

Metabolic pathways were analyzed as described in Xia and Wishart (2010, 2016, using MetaboAnalyst 4.0). Data sets were normalized as described above. Since this analysis is restricted to a two-group comparison the statistics were performed as follows: pathway changes within one exposure group were tested against metabolic status at 14 °C, whilst effects of additional drivers (hypoxia, hypercapnia and the two combined in the deadly trio) were tested against the warming exposure. The pathway library of the zebrafish (*Danio rerio*) was used for pathway identification since most of the profiled metabolites could be assigned to a specific pathway from this library. Further specific statistical methods were 'global test' based on a Bayesian generalized linear model (Goeman et al., 2004) for the determination of global metabolite patterns that are related to specific pathways (pathway enrichment analysis). The importance of a compound/metabolite for a specific metabolic network/pathway (pathway topological analysis) was estimated by a centrality measurement (Aittokallio and Schwikowski, 2006). Identified pathways were checked for plausibility and those identified as being highly uncertain or of false origin were excluded (i.e. pathways with > 30 compounds but only one assigned compound, or pathways associated to specific plant or bacterial metabolism). Residual pathways where considered when associated metabolites displayed significant changes and the pathway was rated by the above mentioned statistical measures with a p-value < .0033 which equals a [-LOG(p)] change > 2.5.

3. Results

3.1. Survival rate

The survival rate of *P. maximus* differed between exposures (Fig. 1). Under warming 82% of scallops were alive at 22 °C. Further warming to 26 °C reduced the number of scallops to 40% indicating that 25 °C is the half-maximal lethal temperature (LC_{50}). All residual scallops died upon transition to 28 °C (T_{Death}). Warming *plus* hypercapnia increased mortality as only 57% of bivalves were still alive at 22 °C and numbers decreased to 50% at 24 °C (LC_{50}). Similar to mortality under W, all scallops died upon transition to 28 °C. Warming *plus* hypoxia led to the same LC_{50} of 24 °C as under WHc. Further warming to 26 °C killed 13 out of 17 residual scallops, leaving four live scallops, which were sacrificed for tissue analysis. Under DT, one fifth of initially introduced scallops died within 48 h after exposure started (14 °C). Warming decreased the number of scallops further, so that at 22.5 °C only half of the scallops were still alive (LC_{50}) and T_{Death} was reached at 28 °C.

3.2. Metabolites

We identified 29 metabolites in phasic muscle with only minor changes between temperatures or exposures. Hence, we focus on gill metabolites and do not show the data set obtained for phasic muscle but cross-refer to these data in the discussion if necessary to draw firmer conclusions.

In gills we identified 34 metabolites with amino acids, amino acid derivates and osmolytes as main compound classes. The metabolic profiles varied with warming and additional treatment (Fig. 2 a/b). Fig. 2a highlights the warming induced changes in metabolite profiles. Warming alone started to alter metabolite profiles at 22 °C resulting in a separation between thermal data clusters and thus, different metabolite profiles between 14 and 26 °C (**W**; Fig. 2a). A similar thermal response was found under additional hypercapnia exposure (**WHc,** Fig. 2a). Under additional hypoxia (**WHo,** Fig. 2a) the metabolic variances between individual scallops of the same sampling temperature decreased but the impact of warming was marginal as all clusters overlap. Similar to WHo combined exposure to all drivers (**DT,** Fig. 2a) caused decreased variances but, in contrast to WHo also resulted in a clear separation between metabolite profiles obtained at 26 °C and those obtained at lower temperatures.

Fig. 2b highlights the treatment induced changes at the different sampling temperatures. With warming the individual variations within the groups decreased as indicated by the declining areas of the confidence ellipses. Thus, at 26 °C metabolite profiles of scallops exposed to DT were clearly separated from those resulting from the other treatments. Significant changes in individual metabolite levels, which underpinned the changes in metabolite profiles outlined above, are depicted according to their metabolite class in Fig. 3 (summary of the statistics is shown in Table 2A). Warming increased the levels of glycine derivate NN-dimethylglycine and acetic acid. NN-dimethylglycine rose from 0.2 ± 0.1 mM at 14 °C to 0.5 ± 0.1 mM at 22 °C (Fig. 3a) while acetic acid concentration was doubled at 26 °C (Fig. 3b). Levels of taurine decreased concomitantly from 64 ± 10.4 mM at 14 °C to 40.2 ± 8.5 mM at 26 °C (Fig. 3c). Additional hypoxia (WHo) affected solely the acetic acid concentration, which increased significantly to its highest value of 0.37 ± 0.012 mM at 18 °C. Concentration was still elevated at 26 °C but it was significantly lower compared to 18 °C. Exposure to warming *plus* hypercapnia (WHc) affected again NN-dimethylglycine and also O-phosphocholine (the latter is only depicted in Table 2A). NN-dimethylglycine concentration was twice as high at 26 °C (0.6 ± 0.01 mM) than at 14 °C (0.3 ± 0.01 mM). Exposure to DT affected the most metabolites. Levels of glycine, NN-dimethylglycine, valine and threonine accumulated at 26 °C. Acetic acid concentration increased significantly at 18 °C and 22 °C and returned to baseline levels at 26 °C. Concomitantly, succinate levels accumulated at 26 °C (from 0.03 ± 0.01 mM at 14 °C to 0.11 ± 0.05 mM at 26 °C).

The differences in metabolite patterns between treatments indicate an impact of additional drivers (Fig. 3, Table 2B). At 14 °C, the concentration of choline, o-phosphocholine, sn-3-glycero-phosphocholine and glycine differed between W and DT. At 18 °C the levels of acetic acid differed between W and WHo and DT, respectively. At 22 °C the concentration of 5 metabolites and at 26 °C of 8 metabolites were altered between exposures. Metabolite levels changed significantly in response to WHo and those changes were in many cases similar to the response to DT. Overall, the majority of significant changes in individual metabolite levels occurred under DT. In contrast, only 3 metabolites differed between W and WHc (o-phosphocholine at 14 °C; acetic acid at 22 °C; NN-dimethylglycine at 26 °C).

3.3. Pathway analysis of gills

Out of 36 putative pathways, seventeen met the selection criteria and 12 pathways were affected by warming with a [-LOG(p)] change > 2.5. Table 3 summarizes pathways that were affected at 26 °C during each exposure. Pathways contributing to carbohydrate metabolism, amino acid metabolism and metabolism of other amino acids were affected by warming. Warming *plus* hypercapnia (WHc) affected amino acid metabolism (as in W) and also lipid metabolism. Warming *plus* hypoxia (WHo) affected two pathways associated with the metabolism of carbohydrates (as in W). Most changes in branchial pathway were observed in scallops exposed to DT with 3 out of 8 pathways involved in amino acid metabolism. Remaining pathways contributed to the conversion of carbohydrates as also seen in scallops under W and WHo exposures.

4. Discussion

We applied untargeted metabolic profiling based on NMR spectroscopy and pathway analysis to identify metabolic and pathway changes in the king scallop, *P. maximus* during exposure to acute warming, additional hypoxia (WHo), additional hypercapnia (WHc) and the combination of all three drivers (Deadly Trio, DT). Overall, hypoxia had a stronger impact than hypercapnia, and effects were even more pronounced in scallops exposed to DT. Gill tissue had characteristic

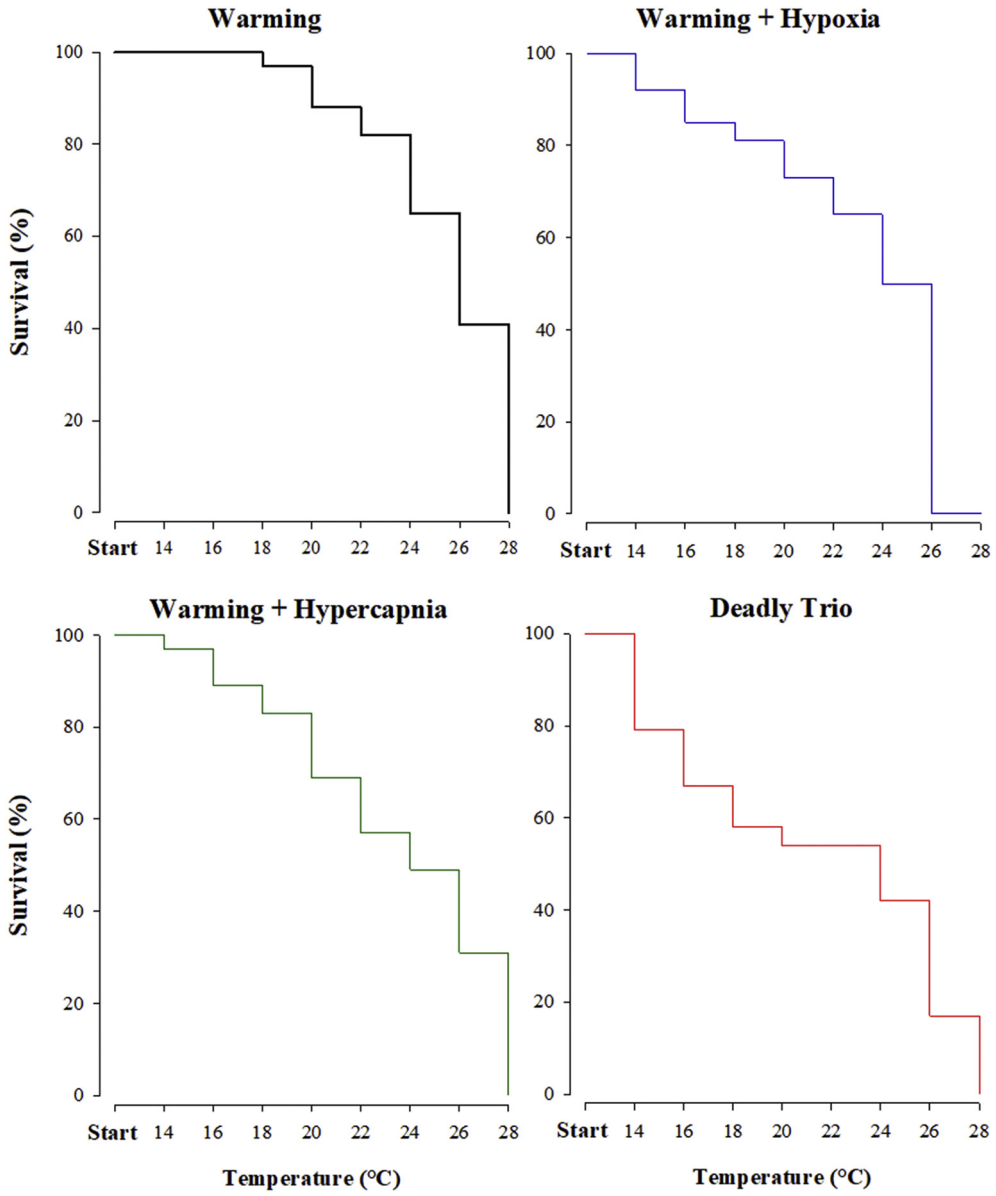

Fig. 1. Survival of *P. maximus* under warming (black), warming *plus* Hypoxia (blue), warming *plus* Hypercapnia (green), and Deadly Trio (warming *plus* Hypoxia *plus* Hypercapnia). The temperature at which 50% of scallops had died (LC_{50}) was reached at 25 °C (W), 24 °C (WHo), 24 °C (WHc), and 22.5 °C (DT). The percentage of surviving scallops is shown for every 2 °C temperature increase. (For interpretation of the references to colour in this figure legend, the reader is referred to the web version of this article.)

metabolic profiles and the metabolic response differed dependent on driver with only few alterations observed during warming and most under DT (as seen at 26 °C). The baseline metabolic profile of gill tissue contained large fractions of free amino acids (e.g. glycine or alanine) and amino acid derivates (such as taurine). This is in line with literature describing the dominant presence of these metabolites in the metabolome of marine invertebrates (Tikunov et al., 2010; Tripp-Valdez et al., 2017; Capello et al., 2018). With respect to their extracellular space marine bivalves are mainly osmoconformers and their cellular osmolality is modulated by the content of compatible solutes such as amino acids (Somero and Yancey, 2011). Accordingly, the main share of metabolites found in *P. maximus* are compatible solutes. Besides their osmotic function they may have further roles as they positively influence for example protein and membrane stability (Rudolph et al., 1986; Rishi et al., 1998; Yancey, 2005). In well-oxygenated gill tissue the main share of energy production comes from oxidative cellular respiration. A study by Hansen et al. (2010) emphasized that taurine concentrations are higher in oxidative than in glycolytic tissue. Indeed, at temperatures within the species' thermal range (10–18 °C) gill tissue had significantly higher taurine concentrations than phasic muscle (14 and 18 °C, $p < .012$; data not shown).

Tissue- as well as species-specific metabolic profiles were identified in various studies (e.g. Tikunov et al., 2010; Hurley-Sanders et al., 2015; Tripp-Valdez et al., 2017; Capello et al., 2018). Some stress assessment studies hypothesized that aerobic tissues such as gills tend to be more sensitive to environmental changes than other organs such as muscle (Lannig et al., 2010; Tripp-Valdez et al., 2017, 2019). Our analysis of phasic muscle tissue of *P. maximus* revealed only few and minor metabolic responses (data not shown), underpinning the particular responsiveness of invertebrate gill tissue.

4.1. *Effects of warming*

Acute warming affected metabolic pathways (Scheme 1). At 22 °C

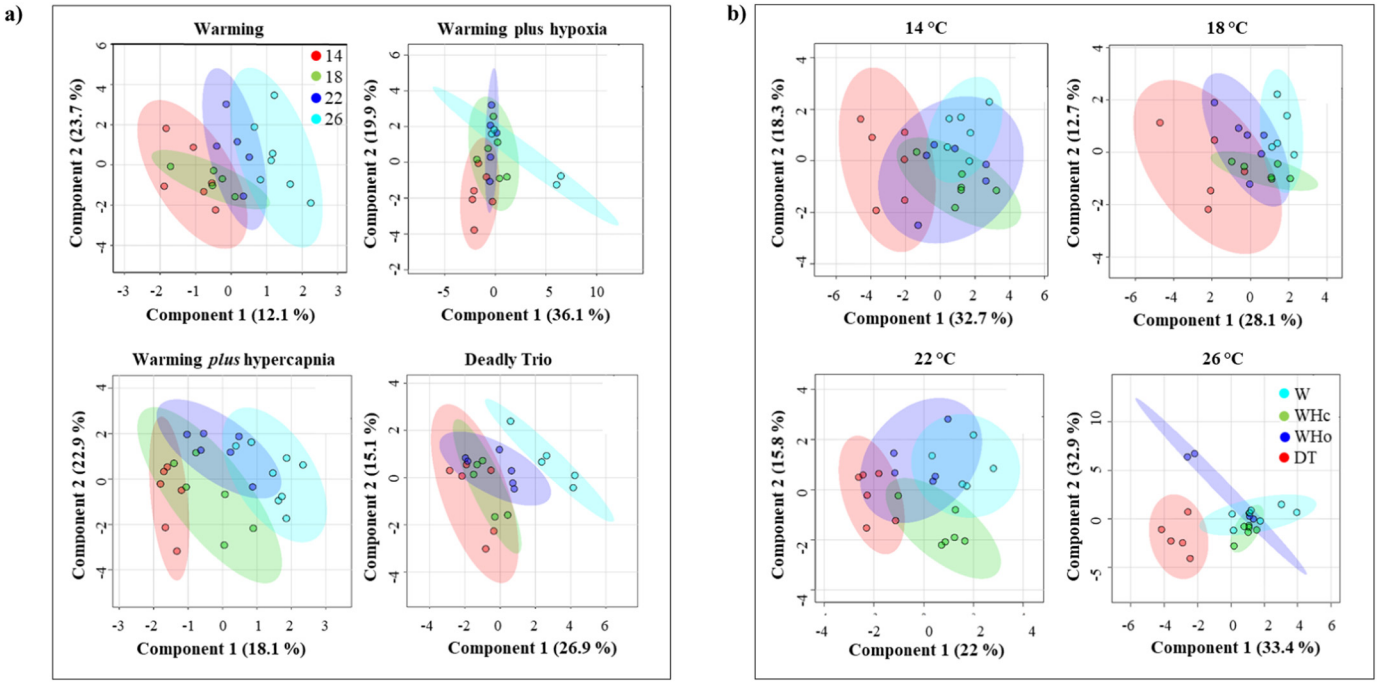

Fig. 2. Impact of the different exposures and sample temperatures on the branchial metabolic profile of *P. maximus*. **a)** Score plots of the PLS-DA model of assigned gill tissue metabolites sampled at 14 °C (red), 18 °C (green), 22 °C (dark blue), and 26 °C (cyan) in the respective exposures. **b)** Score plots assembled according to the respective sample temperature show the differences between branchial metabolic profiles according to the respective exposure group. Warming indicated by light blue, WHc green, WHo dark blue, DT red. Ellipses correspond to a confidence interval of 95%. (For interpretation of the references to colour in this figure legend, the reader is referred to the web version of this article.)

and 26 °C, branchial levels of NN-dimethylglycine increased. This metabolite is a precursor of glycine and has been suggested to be a putative biomarker for starvation in abalone digestive gland tissue (Sheedy et al., 2016). We can exclude starvation as scallops were fed throughout exposures with maximal feeding and filtration efficiencies at 21 °C (Eymann personal comm.). Acetic acid which also was affected is considered to be an end-product of late anaerobiosis (Pörtner and Grieshaber, 1993). It accumulated at 26 °C shortly before the lethal temperature (28 °C) was reached, while succinate, another marker of anaerobiosis (Müller et al., 2012), remained unchanged and accumulated under DT only (see below). Accumulation of acetic acid thus suggests a shift towards anaerobiosis and possibly, a disruption in energy homeostasis. Previous studies investigating the response of *P. maximus* to acute and chronic hyperthermia and hypoxia reported that these scallops thrived below 23 °C (based on condition index and gene expression profiles; Artigaud et al., 2015a) and suggested that scallops switched to anaerobiosis at 25 °C (under both hyperthermia and hypoxia, based on data of octopine dehydrogenase activity and arginine assays; Artigaud et al., 2015b). Finally, warming led to decreasing taurine concentrations at 26 °C. For marine invertebrates taurine often is discussed in the context of osmoregulation. Since we observed only few and random osmolyte changes, we propose that *P. maximus* experienced no osmoregulatory stress in present study. Despite, taurine may function as a pH buffer in the mitochondrial matrix as hypothesized for vertebrates (Hansen et al., 2006, 2010). Furthermore, taurine was found to activate mitochondrial respiration in mouse (Schaffer et al., 2016) which was also shown for an invertebrate, the Pacific oyster (Sokolov and Sokolova, 2019). With respect to its putative role as a mitochondrial buffer or substrate the depletion of taurine might thus, indicate an enhanced mitochondrial respiration or even dysfunction at 26 °C. However, we did not investigate mitochondria metabolism in the context of this study so the consequences of taurine depletion, if any, remain speculative.

4.2. Effects of hypoxia

Our study revealed that gill tissue of *P. maximus* was particularly responsive to hypoxia. Marine water breathers respond to decreasing oxygen tension in the environment. In this context the critical PO_2 reflects the shift from oxyregulation to oxyconformity which is associated with a transition from aerobic towards anaerobic energy production (Pörtner and Grieshaber, 1993). Artigaud et al. (2014) determined the critical PO_2 for *P. maximus* at different temperatures. It increased from 18.3% oxygen saturation at 10 °C to 36.1% oxygen saturation at 25 °C (corresponding to a P_{O2} of 3.9 and 7.6 kPa at 10 °C and 25 °C, respectively, calculated by us). Thus, present hypoxia exposure with P_{O2} values varying between 12.4 and 13.5 kPa (depending on temperature, see Table 1) was above critical levels throughout.

Under warming *plus* hypoxia exposure glycine accumulated and remained elevated during progressive warming, paralleled by an accumulation of acetic acid and acetoacetate (significantly higher at 26 °C during WHo than W exposure; Scheme 2a). Glycogenic amino acids such as glycine have multiple cellular functions as they e.g. serve as osmolytes, promote protein synthesis, or are used for energy production via glycolysis (Ellis et al., 1985; Wang et al., 2013). 'Stressed cells' switch to pronounced protein catabolism and exploit among others glycogenic amino acids to fuel energy metabolism (e.g. Salway, 2004). Levels of alanine, glycine, or arginine were also elevated in abalone in response to environmental hypoxia (Tripp-Valdez et al., 2017; Venter et al., 2018). Together with the accumulation of acetic acid the observed changes suggest alterations in branchial energy metabolism in *P. maximus*. This is further supported by the putative mobilization of lipid energy reserves via ß-oxidation of acetoacetate (Table 2B). The concentration of this metabolite did not change with warming but was significantly higher in scallops exposed to either WHo or DT at 26 °C pointing to a pronounced energetic demand. Interestingly, increasing acetylcarnitine levels in phasic muscle (from 0.019 ± 0.007 mM at 14 °C to 0.054 ± 0.018 mM at 22 °C, $p = .002$, data not shown) also suggest an increase in fatty acid oxidation in line with the hypothesized

a) Amino Acids and derivates

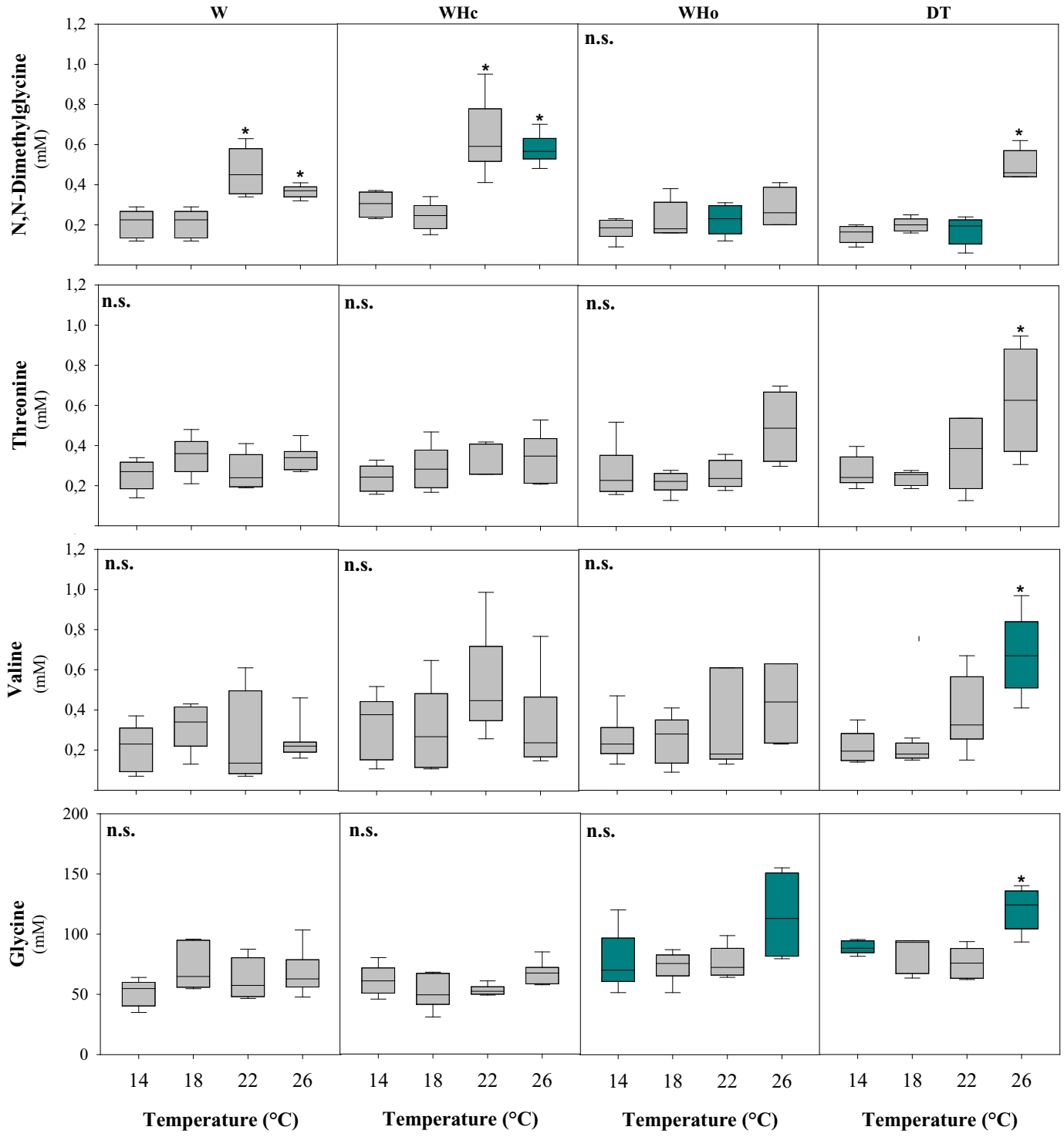

Fig. 3. Metabolite levels in gill tissue of *P. maximus*. **a)** amino acids **b)** metabolites related to energy metabolism **c)** osmolytes. Data are mean, normalized concentrations as mM ± SD, n = 5–8 (expect n = 4 at 26 °C WHo). Asterisks mark significant differences to concentrations at 14 °C. Colored bars indicate that the metabolite concentration was significantly different from the group sampled after warming to this temperature.

enhanced branchial energetic need. Artigaud and coworkers investigated the molecular adaptation of *P. maximus* to heat stress (2015a, 2015b). After exposure to 25 °C for 56 days an upregulation of genes in the mantle was observed associated with lipid metabolism coinciding with a decrease in condition and explained their findings by the need of *P. maximus* to meet the increasing metabolic demand at this temperature.

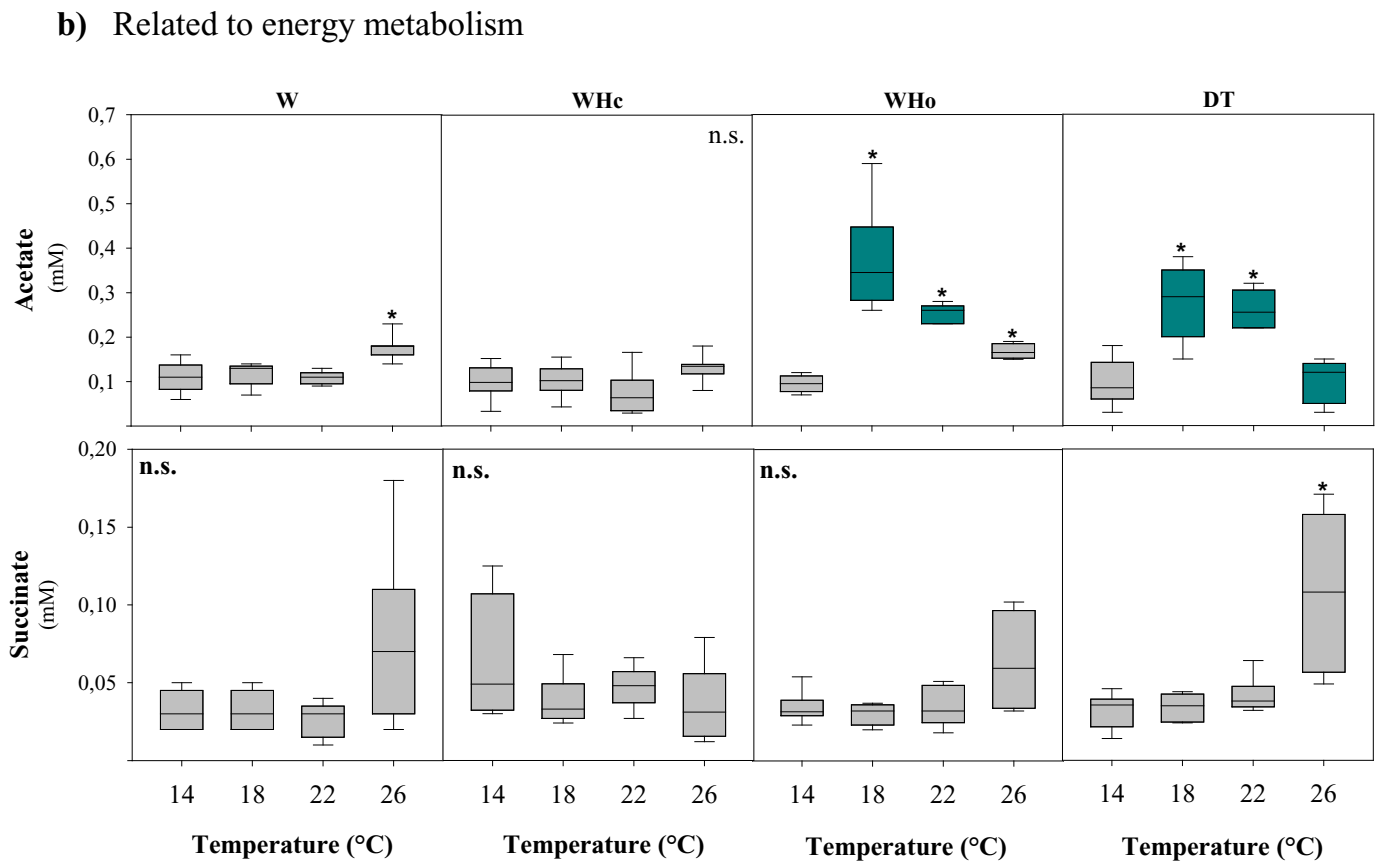

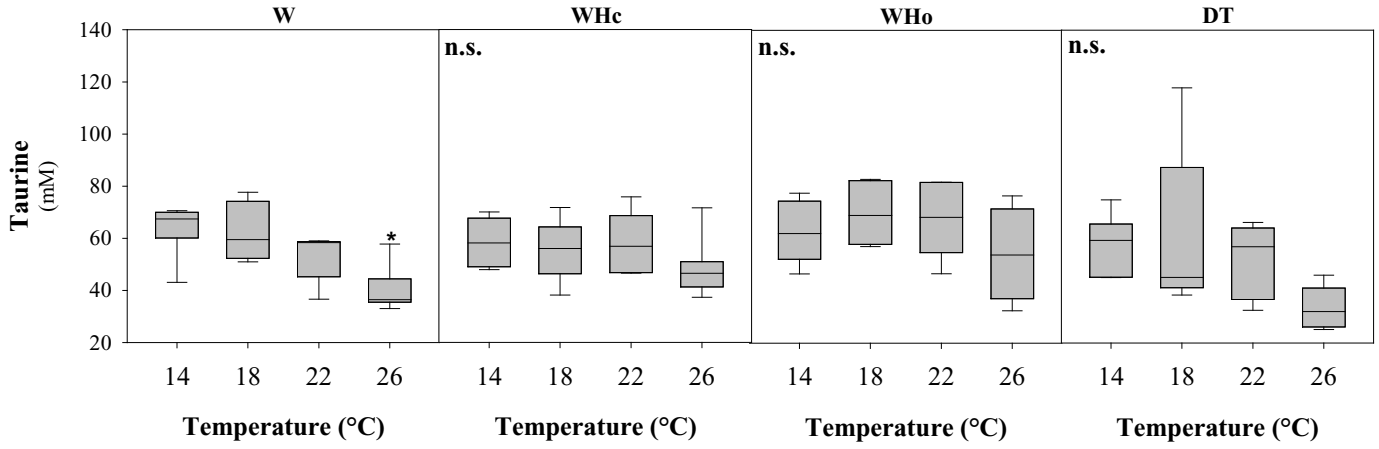

Fig. 3. (*continued*)

4.3. Effects of hypercapnia

Acute hypercapnia on top of warming had the lowest impact on branchial metabolism of *P. maximus* (Scheme 2b). NN-dimethylglycine and O-phosphocholine levels accumulated (Table 2A) with unclear biological function of dimethylglycine (see discussion above). O-phosphocholine is an intermediate needed for the synthesis of phosphatidylcholine which by itself is an important component of cell membranes (Kraffe et al., 2004). Both warming and hypercapnia, can alter the lipid composition of cell membranes (Strobel et al., 2013; Valles-Regino et al., 2015), endanger cell membrane homeostasis by the oxidation of lipids, or affect acid-base homeostasis (Wittmann and Pörtner, 2013). Previous studies on temperate and boreal *P. maximus* (Schalkhausser et al., 2013; Schalkhausser et al., 2014) showed that the capacity to maintain acid-base homeostasis was higher in temperate than boreal specimens explaining why the temperate population was more tolerant towards hypercapnia. The observed low impact of WHc on gill metabolism and organism survival in present study on temperate *P. maximus* from Galicia (Spain) also suggests that this population is tolerant to environmental hypercapnia.

Table 2A
Results of one-way ANOVA for significant changes in gill metabolite levels tested against a) temperature. Shown is the compound, the f-value, *p*-value, [-LOG10(p)], and the resulting Fisher' LSD.

Compound	F-value	P-value	[-LOG10(p)]	Fisher's LSD
Warming				
NN Dimethylglycine	15,0	3,0E-05	4,5	14, 18 < 22, 26
Taurine	8,5	8,7E-04	3,1	14, 18, 22 > 26
Acetic acid	6,9	2,5E-03	2,6	14–22 < 26
Hypercapnia				
NN Dimethylglycine	17,0	6,2E-06	5,2	14, 18 < 22, 26
O-Phosphocholine	7,0	1,7E-03	2,8	14, 18, 22 < 26
Hypoxia				
Acetic acid	35,2	1,6E-07	6,8	14 < 18–26; 18 > 26
Deadly Trio				
NN Dimethylglycine	13,3	8,2E-05	4,1	14–22 < 26
Succinate	11,6	1,8E-04	3,7	14–22 < 26
Valine	11,5	1,9E-04	3,7	14, 18 < 22, 26; 22 < 26
Acetic acid	9,8	4,7E-04	3,3	14 < 18, 22; 18, 22 > 26
Glycine	9,6	5,2E-04	3,3	14–22 < 26
Threonine	5,2	9,0E-03	2,0	14–22 < 26

Table 2B
Results of one-way ANOVA for significant changes in gill metabolite levels tested against exposure. Shown is the compound, the f-value, p-value, [-LOG10(p)], and the resulted Fisher' LSD.

Compound	F-value	P-value	[-LOG10(p)]	Fisher's LSD
14 °C				
Choline	15,1	2,3E-05	4,6	W - DT
O-Phosphocholine	13,7	4,3E-05	4,4	W - HO, HC, DT
sn-Glycero-3-phosphocholine	7,9	1,1E-03	2,9	W - DT
Glycine	6,4	3,3E-03	2,5	W - HO, DT
18 °C				
Acetic acid	20,1	5,7E-06	5,2	W - HO, DT
22 °C				
Acetic acid	23,3	2,0E-06	5,7	W - HO, HC, DT
Choline	13,6	7,0E-05	4,2	W - DT
NN Dimethylglycine	12,6	1,1E-04	3,9	W - HO, DT
O-Phosphocholine	9,3	6,2E-04	3,2	W - DT
Dimethysulfone	8,3	1,2E-03	2,9	W - HO
26 °C				
Acetoacetate	13,8	5,1E-05	4,3	W - HO; DT
Choline	12,8	8,1E-05	4,1	W - DT
Glycine	11,4	1,7E-04	3,8	W - HO, DT
Dimethysulfone	7,5	1,6E-03	2,8	W - HO, DT
Trigonelline	6,8	2,7E-03	2,6	W - HO, DT
NN Dimethylglycine	5,8	5,4E-03	2,3	W - HC
Acetic acid	5,6	6,1E-03	2,2	W - DT
Valine	5,4	7,3E-03	2,1	W - DT

4.4. Effects of deadly trio

Simultaneous exposure to all three drivers most severely affected branchial metabolism (Scheme 2c). The use of metabolic pathways was consistent between individual scallops likely indicating that DT exposure constrains the metabolic response in a certain direction. This is in line with observations under WHo exposure, suggesting that WHo acts as the key underlying driving force. However, the metabolic response was more uniform under WHo than under DT. This may be the result of a stimulatory effect of hypercapnia under DT, as suggested earlier in mollusks (e.g. Zittier et al., 2015; Tripp-Valdez et al., 2017). Immediately after the onset of DT exposure the branchial levels of glycine increased indicating a cellular stress response similar to that under hypoxia (see discussion above). Most likely, glycine originated

Table 3
Significant changes in gill metabolic pathways with a [-LOG(p)] change of > 2.5. As a reference metabolic pathways of the zebrafish (*Danio rerio*) were chosen. Shown is the pathway including the total number of compounds, the number and names of the identified hits, the raw p-value, the [-LOG(p)] change, as well as Holm adjust, FDR, and IMP. Metabolites written in bold indicate a significant change determined in the ANOVA.

14 vs.26 °C	Pathway	Incr/Decr	Total Cmpd	Hits	Compounds identified in the pathway	Raw p	[-LOG(p)]	Holm adjust	FDR	IMP
Warming										
Carbohydrate metabolism	Pyruvate metabolism	↑	22	1	Acetic acid	2E-03	6,1	0,1	0,0	0,1
	Glycolysis or Gluconeogenesis	↑	26	1	Acetic acid	2E-03	6,1	0,1	0,0	0,0
Amino acid metabolism	Glycine, serine and threonine metabolism	↑	31	6	Choline, Threonine - Glycine - Sarcosine, Betaine - Dimethylglycine	8E-03	4,8	0,3	0,1	0,3
Metabolism of other Amino acids	Taurine and hypotaurine metabolism	↓	7	2	Taurine, Hypotaurine	4E-02	3,1	1,0	0,2	0,5
Warming + Hypercapnia										
Amino acid metabolism	Glycine, serine and threonine metabolism	↑	31	6	Choline, Threonine - Glycine - Sarcosine, Betaine - Dimethylglycine	2E-02	4,0	0,6	0,0	0,3
Lipid metabolism	Glycerophospholipid metabolism	↑	27	3	Glycerophosphocholine, Choline - Phosphocholine	2E-02	3,9	0,6	0,0	0,1
Warming + Hypoxia										
Carbohydrate metabolism	Pyruvate metabolism	↑	22	1	Acetic acid	2E-03	6,2	0,1	0,03	0,08
	Glycolysis or Gluconeogenesis	↑	26	1	Acetic acid	2E-03	6,2	0,1	0,03	0,03
Deadly Trio										
Amino acid metabolism	Glycine, serine and threonine metabolism	↑	31	6	Choline, Threonine - Glycine - Sarcosine, Betaine - Dimethylglycine	7E-07	14,2	0,0	0,0	0,3
Carbohydrate metabolism	Butanoate metabolism	↑	22	3	Glutamate, Succinate, Acetoacetate	5E-04	7,6	0,0	0,0	0,1
Amino acid metabolism	Valine, leucine and isoleucine biosynthesis	↑	13	4	Valine, Leucine, Isoleucine, Threonine	8E-04	7,1	0,0	0,0	1,0
Carbohydrate metabolism	Propanoate metabolism	↑	20	2	Succinate, ß-Alanine	9E-04	7,0	0,0	0,0	0,0
Amino acid metabolism	Alanine, aspartate and glutamate metabolism	↑	24	5	Aspartate, Alanine, Glutamate - Glutamine, Succinate	1E-03	6,8	0,0	0,0	0,6
Carbohydrate metabolism	Citrate cycle (TCA cycle)	↑	20	1	Succinate	1E-03	6,7	0,0	0,0	0,0
Amino acid metabolism	Valine, leucine and isoleucine degradation	↑	38	4	Valine, Leucine, Isoleucine, Acetoacetate	2E-03	6,3	0,1	0,0	0,0
Metabolism of other Amino acids	Glutathione metabolism	↑	26	2	Glycine, Glutamate	5E-02	2,9	1,0	0,1	0,0

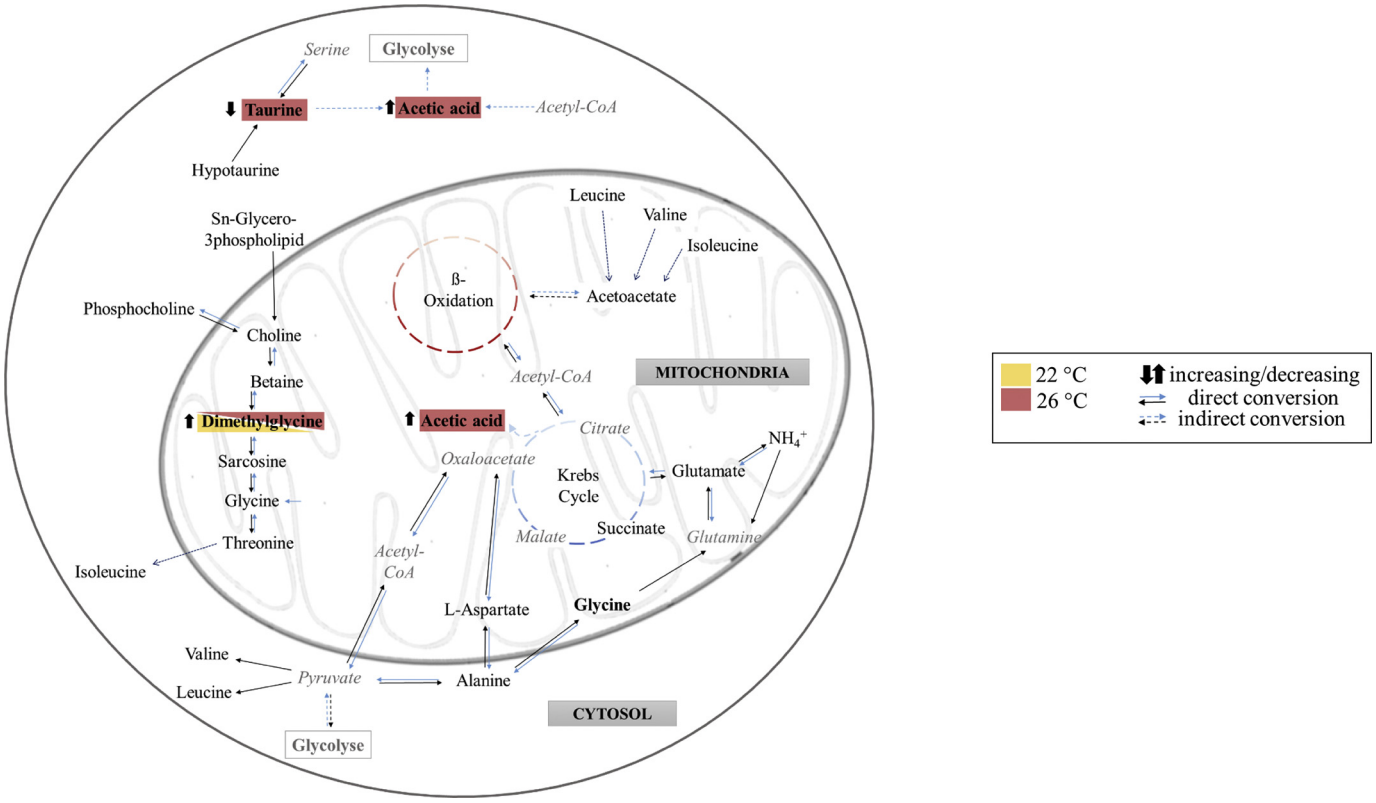

Scheme 1. Assigned metabolites found in gills of *P. maximus* exposed to acute warming. Metabolites in bold indicate significant changes in metabolite levels, while grey and italic metabolites are not assigned intermediates of the pathway. Metabolite names in colored boxes code for the sampling temperature (orange 22 °C and red 26 °C). Arrows indicate an increase (up) or decrease (down) of the respective metabolite concentration

from protein degradation and was catabolized further for glycolytic energy production. Altered metabolite patterns of choline, phosphocholine and sn-glycero-3-phospholipid (compared to W, Table 2B) suggest that cellular membrane integrity might be affected, as all three metabolites are involved in cell membrane homeostasis (see above; reviews by Ernst et al., 2016; Harayama and Riezman, 2018).

The switch from acetic acid accumulation (at 18 °C and 22 °C) to succinate accumulation (at 26 °C) may be indicative of more pronounced alterations in mitochondrial energy metabolism at temperatures ≥18 under DT exposure than the other exposures. The contrasting changes in acetic acid and succinate concentrations suggest that Co-A may be transferred from succinyl-CoA to acetic acid by acetic acid:succinate CoA-transferase causing the accumulation of succinate (Müller et al., 2012). In combination with the observed drop in whole animal respiration at 22 °C under DT exposure (Eymann personal comm.) the present data support the hypothesis that temperature

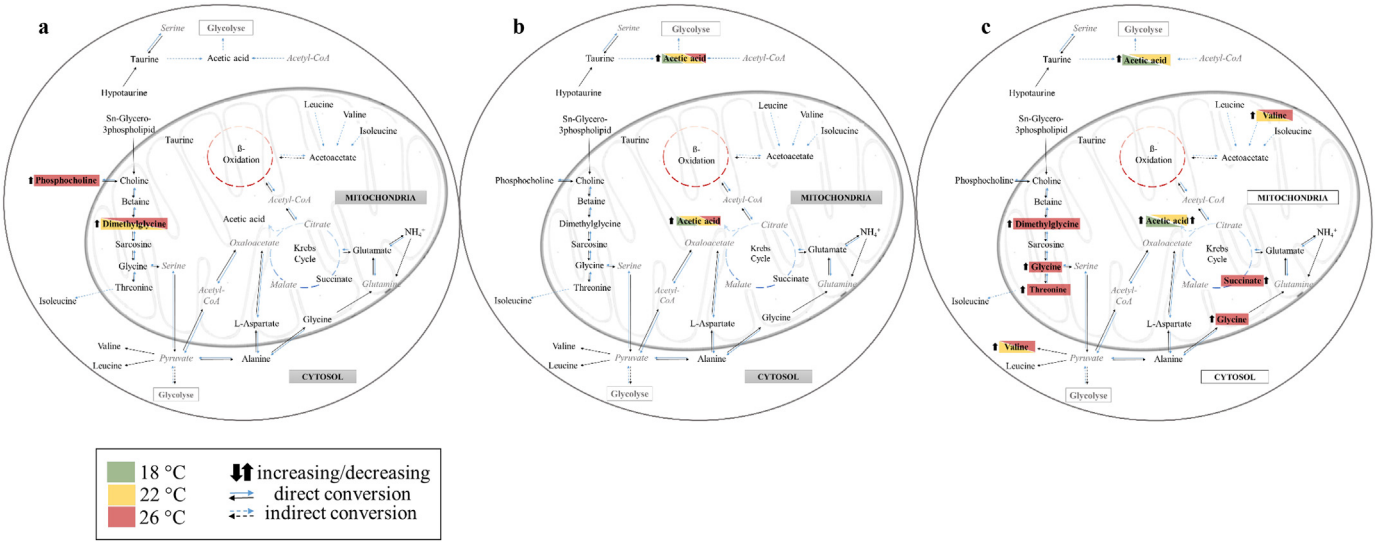

Scheme 2. Assigned branchial metabolites of *P. maximus* exposed to acute WHc (**a**), WHo (**b**), and DT (**c**). Metabolites in bold indicate significant changes in metabolite levels, while grey and italic metabolites are not assigned intermediates of the pathway. Metabolite names in colored boxes code for the temperature (green 18 °C, orange 22 °C, red 26 °C). Arrows indicate an increase (up) or decrease (down) of the respective metabolite concentration.

dependent limitation in oxygen supply paralleled by an acceleration of cellular metabolic rates may have led to a severe mismatch between energy demand and supply according to the concept of oxygen and capacity limited thermal tolerance (OCLTT; Pörtner et al., 2017), as a potential mechanism decreasing the upper limit of thermal tolerance. This is in line with findings of Tripp-Valdez et al. (2017). After combined exposure to warming, hypoxia and hypercapnia of juvenile green abalone (*Haliotis fulgens*; + 3 °C per day; 50% O_2; ~1000 µatm pCO_2) animals showed a strongly perturbed energy metabolism at higher temperatures, indicated by an early onset of anaerobiosis (accumulation of anaerobic end products and glycogenic amino acids) and T*c* and CT_{max} were reached at lower temperatures than under warming alone.

4.5. Transfer to the field and outlook

Temperature has an overarching impact on an animal's physiology and aerobic performance and, thus, shapes the fundamental niche of a species (Somero, 2002; Pörtner et al., 2017) and building on that, its realized niche (Pörtner et al., 2017). Metabolic responses to acute warming were altered by additional exposures, in particular to hypoxia and DT as indicated by shifts in mitochondrial energy metabolism at lower temperatures. Most severe changes were observed under DT lowering the upper thermal limit visible by enhanced mortality and lowered LC_{50} (from 25 °C in W to 22.5 °C in DT). In contrast to other bivalves such as mussels or oysters, the scallop's lifestyle might reflect an evolutionary trade-off. The capacity to be alert and ready to swim seems not to select for a high capacity in metabolic depression (reduction of standard metabolic rate; SMR) or tolerance to oxygen depletion (shut close and outlive unfavorable conditions). Indeed, scallops maintain higher PO_2 levels in the mantle cavity correlating with a higher SMR compared to sessile mud clams (Abele et al., 2010). Accordingly, ongoing global warming combined with the expansion of oxygen-depleted hypercapnic water layers might have negative consequences for the scallops' survival.

These relationships may have also been decisive when pectinid ancestors were exposed to rapid and extreme changes of environmental conditions during past marine crises. While ancient bivalves in general were one of the less affected groups during the PTME with a fast recovery rate (Fraiser and Bottjer, 2007), the huge loss of oxygenated habitats in combination with warming might have had severe consequences for some of them, as indicated by the extinction patterns of ancient scallops. Tu et al. (2016) investigated extinction and recovery patterns from the Changhsingian (latest Permian) to Anisian (Middle Triassic) and reported that pectinida (together with myalinida and pholadomyida) were stronger affected than ostreida or mytilida. In line with findings of Penn et al. (2018) who stated that once present climate changes reach the same dimensions as during the Permian-Triassic, modern *P. maximus* would lose up to 100% of their habitat. While some aspects explaining the particular vulnerability of pectinids are emerging, further studies are needed to fully exploit the mechanisms that are involved in shaping vulnerability to environmental change.

Declaration of Competing Interest

The authors declare that they have no known competing financial interests or personal relationships that could have appeared to influence the work reported in this paper.

Acknowledgments

The study was funded by the Deutsche Forschungsgemeinschaft (Po278/16-1) and is part of the Research Unit TERSANE (FO 2332). We thank Anette Tillman, Lea Philipps, and Timo Hirse for the analysis of water quality and concentrations of dissolved inorganic carbon. Martin Aberhan for helpful discussion of the evolution of bivalves and mass extinction events and Inna Sokolova for the discussion of biochemical pathways. We thank the Biological station of Toralla (ECIMAT, Spain), in particular A. Villanueva and D. Costas for support in animal supply and F. Feliz Moraleda for animal care.

Appendix A. Supplementary data

Supplementary data to this article can be found online at https://doi.org/10.1016/j.cbpb.2020.110438.

References

Abele, D., Kruppe, M., Philipp, E.E.R., Brey, T., 2010. Mantle cavity water oxygen partial pressure (PO_2) in marine molluscs aligns with lifestyle. Can. J. Fish. Aquat. Sci. 67, 977–986. https://doi.org/10.1139/F10-035.

Aberhan, M., Baumiller, T., 2003. Selective extinction among Early Jurassic bivalves: a consequence of anoxia. J. Geol. 31, 1077–1080. https://doi.org/10.1130/G19938.1.

Aittokallio, T., Schwikowski, B., 2006. Graph-based methods for analysing networks in cell biology. Brief. Bioinform. 7, 243–255. https://doi.org/10.1093/bib/bbl022.

Artigaud, S., Lacroic, C., Pichereau, V., Flye-Sainte-Marie, J., 2014. Respiratory response to combined heat and hypoxia in the marine bivalves *Pecten maximus* and *Mytilis spp*. Comp. Biochem. Physiol. A 175, 135–140. https://doi.org/10.1016/j.cbpa.2014.06.005.

Artigaud, S., Richard, J., Thorne, M.A.S., Lavaud, R., Flye-Sainte-Marie, J., Jean, F., Peck, L.S., Clark, M.S., Pichereau, V., 2015a. Deciphering the molecular adaption of the king scallop (*Pecten maximus*) to heat stress using transcriptomics and proteomics. BMC Genomics 16, 988. https://doi.org/10.1186/s12864-015-2132-x.

Artigaud, S., Lacroix, C.C.L., Richard, J.J.R., Flye-Sainte-Marie, J., Bargelloni, L.L.B., Pichereau, V., 2015b. Proteomic responses to hypoxia at different temperatures in the great scallop (*Pecten maximus*). PeerJ 3, e871. https://doi.org/10.7717/peerj.871.

Bachan, A., Payne, J.L., 2015. Modelling the impact of pulsed CAMP volcanism of PCO_2 and $^{\delta}13C$ across the Triassic-Jurassic transition. Geol. Mag. 153, 252–270. https://doi.org/10.1017/S0016756815000126.

Bambach, R.K., Knoll, A.H., Wang, S.C., 2004. Origination, extinction, and mass depletions of marine diversity. Paleobiology 30, 522–542.

Bock, C., Wermter, F., Schalkhausser, B., Blicher, M.E., Pörtner, H.O., Lannig, G., Sejr, M.K., 2019. In vivo 31P-MRS of muscle bioenergetics in marine invertebrates: future Ocean limits scallops' performance. Magn. Reson. Imaging 61, 239–246. https://doi.org/10.1016/j.mri.2019.06.003.

Breitburg, D., Levin, L.A., Oschlies, A., Grégoire, M., Chavez, F.P., Conley, D.J., Garçon, V., Gilbert, D., Gutiérrez, D., Isensee, K., Jacinto, G.S., Limburg, K.E., Montes, I., Naqvi, S.W.A., Pitcher, G.C., Rabalais, N.N., Roman, M.R., Rose, K.A., Seibel, B.A., Telszewski, M., Yasuhara, M., Zhang, J., 2018. Declining oxygen in the global ocean and coastal waters. Science 359. https://doi.org/10.1126/science.aam7240.

Capello, T., Giannetto, A., Parrino, V., Maisano, M., Olivia, S., De Marco, G., Guerriero, G., Mauceri, A., Fasulo, S., 2018. Baseline levels of metabolites in different tissues of mussel *Mytilus galloprovincialis* (Bivalvia: Mytilidae). Comp. Physiol. D 26, 32–39. https://doi.org/10.1016/j.cbd.2018.03.005.

Clarkson, M.O., Kasemann, S.A., Wood, R.A., Lenton, T.M., Daines, S.J., Richoz, S., Ohnemueller, F., Meixner, A., Poulton, W., Tipper, T., 2015. Ocean acidification and the Permo-Triassic mass extinction. Science 348, 229–232.

Diaz, R.J., Rosenberg, R., 2008. Spreading Dead Zones and consequences for marine ecosystems. Science 321, 926–929.

Ellis, L.L., Burcham, J.M., Paynter, K.T., Bishop, S.H., 1985. Amino acid metabolism in euryhaline bivalves. Regulation of glycine accumulation in ribbed mussel gills. J. Exp. Zool. 233, 347–358. https://doi.org/10.1002/jez.1402330303.

Ellis, R.P., Spicer, J.I., Byrne, J.J., Sommer, U., Viant, M.R., White, D.A., Widdicombe, S., 2014. ^{1}H NMR metabolomics reveals contrasting response by male and female mussels exposed to reduced seawater pH, increased temperature, and a pathogen. Environ. Sci. Technol. 48, 7044–7052. https://doi.org/10.1021/es501601w.

Ern, R., Johansen, J.L., Rummer, J.L., Esbaugh, A., 2017. Effects of hypoxia and ocean acidification on the upper thermal niche boundaries of coral reef fishes. Biol. Lett. 13https://doi.org/10.1098/rsbl.2017.0135. 20170135.

Ernst, R., Ejsing, C.S., Antonny, B., 2016. Homeoviscous adaptation and the regulation of membrane lipids. J. Mol. Biol. 24, 4776–4791. https://doi.org/10.1016/j.jmb.2016.08.013.

Eymann, C., Götze, S., Bock, C., Guderley, H., Knoll, A.H., Lannig, G., Sokolova, I., Aberhan, M., Pörtner, H.O., 2020. Thermal performance of the European flat oyster, *Ostrea edulis* (Linnaeus, 1758) – explaining ecological findings under climate change. Mar. Biol. 167, 7. https://doi.org/10.1007/s00227-019-3620-3.

Fraiser, M.L., Bottjer, D.J., 2007. When bivalves took over the world. Palaeobiology 33, 397–413.

Goeman, J.J., Van de Geer, S.A., De Kort, F., Houwellingen, H.C., 2004. A global test for groups of genes: testing association with a clinical outcome. Bioinformatics 20, 93–99. https://doi.org/10.1093/bioinformatics/btg382.

Grieshaber, M., 1978. Breakdown and formation of high-energy phosphates and octopine in the adductor muscle of the scallops, *Chlamys opercularis* (L.), during escape swimming and recovery. J. Comp. Physiol. 126, 269–276. https://doi.org/10.1007/BF00688937.

Guderley, H., Pörtner, H.O., 2010. Metabolic power budgeting and adaptive strategies in zoology: examples from scallops and fish. Can. J. Zool. 88, 753–763. https://doi.org/10.1139/Z10-039.

Guinotte, J.M., Fabry, V.J., 2008. Ocean acidification and its potential effects on marine ecosystems. Ann. N. Y. Acad. Sci. 1134, 320–342. https://doi.org/10.1196/annals.1439.013.

Hansen, S.H., Andersen, M.L., Birkedal, H., Cornett, C., Wibrand, F., 2006. The important role of taurine in oxidative metabolism. In: Oja, S.S., Saransaari, P. (Eds.), Taurine 6. Advances in Experimental Medicine and Biology. vol 583 Springer, Boston, MA. https://doi.org/10.1007/978-0-387-33504-9_13.

Hansen, S.H., Andersen, M.L., Cornett, C., Gradinaru, R., Grunnet, N., 2010. A role for taurine in mitochondrial function. J. Biomed. Sci. 17. https://doi.org/10.1186/1423-0127-17-S1-S23.

Harayama, T., Riezman, H., 2018. Understanding the diversity of membrane lipid composition. Nature reviews. Mol. Cell. Biol. 19, 281–296. https://doi.org/10.1038/nrm.2017.138.

Heise, K., Puntarulo, S., Pörtner, H.O., Abele, D., 2003. Production of reactive oxygen species by isolated mitochondria of the Antarctic bivalve *Laternula elliptica* (King and Broderip) under heat stress. Comp. Biochem. Physiol. C 134, 79–90. https://doi.org/10.1016/S1532-0456(02)00212-0.

Heise, K., Puntarulo, S., Nikinmaa, M., Abele, D., Pörtner, H.O., 2006. Oxidative stress during stressful heat exposure and recovery in the North Sea eelpout *Zoarces viviparus* L. J. Exp. Biol. 209, 353–363. https://doi.org/10.1242/jeb.01977.

Hurley-Sanders, J.L.H., Levine, J.F., Nelson, S.A.C., Law, J.M., Showers, W.J., Stoskopf, M.K., 2015. Key metabolites in tissue extracts of *Elliptio complanata* identified using ^{1}H nuclear magnetic resonance spectroscopy. Conserv. Physiol. 3https://doi.org/10.1093/conphys/cov023. cov023.

IPCC, 2019. Summary for Policymakers. In: Pörtner, H.-O., Roberts, D.C., Masson-Delmotte, V., Zhai, P., Tignor, M., Poloczanska, E. ... Weyer, N.M. (Eds.), IPCC Special Report on the Ocean and Cryosphere in a Changing Climate, In press. https://www.ipcc.ch/srocc/chapter/summary-for-policymakers/.

Joachimski, M.M., Lai, X., Shen, S., Jiang, H., Luo, G., Chen, B., Chen, J., Sun, Y., 2012. Climate warming in the latest Permian and the Permian–Triassic mass extinction. Geology 40, 195–198.

Jones, O.A., Dondero, F., Viarengo, A., Griffin, J.L., 2008. Metabolic profiling of *Mytilus galloprovincialis* and its potential applications for pollution assessment. Mar. Ecol. Prog. Ser. 369, 169–179. https://doi.org/10.3354/meps07654.

Kassahn, K.S., Crozier, R.H., Pörtner, H.O., Caley, M.J., 2009. Animal performance and stress: responses and tolerance limits at different levels of biological organization. Biol. Rev. 84, 277–292. https://doi.org/10.1111/j.1469-185X.2008.00073.x.

Keeling, R.F., Körtzinger, A., Gruber, N., 2010. Ocean deoxygenation in a warming world. Annual Review of Mar. Sci. 2, 199–229.

Kraffe, E., Soudant, P., Marty, Y., 2004. Fatty acids of serine, ethanoamine, and choline plasmogens in some marine bivalves. Lipids 39, 59–66. https://doi.org/10.1007/s11745-004-1202-x.

Laing, I., 2000. Effect of temperature and ration on growth and condition of king scallop (*Pecten maximus*) spat. Aquaculture 183, 325–334. https://doi.org/10.1016/S0044-8486(99)00262-8.

Lannig, G., Eilers, S., Pörtner, H.O., Sokolova, I., Bock, C., 2010. Impact of Ocean acidification on energy metabolism of oyster, *Crassostrea gigas* – Changes in metabolic pathways and thermal response. Mar. Drugs 8, 2318–2339. https://doi.org/10.3390/md8082318.

Laudien, J., Schiedek, D., Brey, T., Pörtner, H.O., Arntz, W.E., 2002. Survivorship of juvenile surf clams *Donax serra* (Bivalvia, Donacidae) exposed to severe hypoxia and hydrogen sulphide. J. Mar. Biol. Ecol. 1, 9–23. https://doi.org/10.1016/S0022-0981(02)00030-8.

Lau, K.V., Maher, K., Altinen, D., Kelley, B.M., Kump, L.R., Lehrmann, D.J., Silva-Tamayo, J.C., Weaver, K.L., Yu, M., Payne, J.L., 2016. Marine anoxia and delayed Earth system recovery after the end-Permian extinction. PNAS 113, 2360–2365.

Lenz, E.M., Weeks, J.M., Lindon, J.C., Osborn, D., Nicholson, J.K., 2005. Qualitative high field ^{1}H-NMR spectroscopy for the characterization of endogenous metabolites in earthworms with biochemical biomarker potential. Metabolomics 1, 123–136. https://doi.org/10.1007/s11306-005-4435-4.

Müller, M., Mentel, M., van Hellemond, J.J., Henze, K., Woehle, C., Gould, S.B., Yu, R.-Y., van der Giezen, M., Tielens, A.G.M., Martin, W.F., 2012. Biochemistry and evolution of anaerobic energy metabolism in eukaryotes. Microbiol. Mol. Biol. Rev. 76, 444–495. https://doi.org/10.1128/MMBR.05024-11.

Palma, P.F.S., Bock, C., Silva, T.S., Guerreiro, P.M., Power, D.M., Pörtner, H.O., Canario, A.V.M., 2019. STC1 and PTHrP modify carbohydrate and lipid metabolism in liver of a teleost fish. Sci. Rep. 9. https://doi.org/10.1038/s41598-018-36821-2.

Parker, L.M., Ross, R.M., O'Connor, W.A., Pörtner, H.O., Scanes, E., Wright, J.M., 2013. Predicting the response of molluscs to the impact of ocean acidification. Biology 2, 651–692. https://doi.org/10.3390/biology2020651.

Penn, J.L., Deutsch, C., Payne, J.L., Sperling, E.A., 2018. Temperature-dependent hypoxia explains biogeography and severity of end-Permian marine mass extinction. Science 362 (6419). https://doi.org/10.1126/science.aat1327.

Pörtner, H.O., 2002. Climate variations and the physiological basis of temperature dependent biogeography: systemic to molecular hierarchy of thermal tolerance in animals. Comp. Biochem. Physiol. A 132, 739–761. https://doi.org/10.1016/S1095-6433(02)00045-4.

Pörtner, H.O., 2012. Integrating climate-related stressors effects on marine organisms: unifying principles linking molecule to ecosystem-level changes. Mar. Ecol. Prog. Ser. 470, 273–290. https://doi.org/10.3354/meps10123.

Pörtner, H.O., Grieshaber, M.K., 1993. Characteristics of the critical PO 2 (s): gas exchange, metabolic rate and the mode of energy production. In: Bicudo, J.E.P.W. (Ed.), The Vertebrate Gas Transport Cascade: Adaptations to Environment and Mode of Life. CRC Press Inc., Boca Raton (FL), U.S.A, pp. 330–357.

Pörtner, H.O., Langenbuch, M., Reipschläger, A., 2004. Biological impact of elevated ocean CO_2 concentrations: lessons from animal physiology and earth history. J. Oceanogr. 60, 705–718. https://doi.org/10.1007/s10872-004-5763-0.

Pörtner, H.O., Bock, C., Mark, F.C., 2017. Oxygen-and capacity-limited thermal tolerance: bridging ecology and physiology. J. Exp. Biol. 220, 2685–2696. https://doi.org/10.1242/jeb.134585.

Purohit, P.V., Rocke, D.M., Viant, M.R., Woodruff, D.L., 2004. Discrimination models using variance-stabilizing transformation of metabolomic NMR data. Omics 8, 118–130. https://doi.org/10.1089/1536231041388348.

Rebelein, A., Pörtner, H.O., Bock, C., 2018. Untargeted metabolic profiling reveals distinct patterns of thermal sensitivity in two related notothenioids. Comp. Biochem. Physiol. A 217, 43–54. https://doi.org/10.1016/j.cbpa.2017.12.012.

Rishi, V., Anjum, F., Ahmad, F., Pfeil, W., 1998. Role of-compatible osmolytes in the stabilization of proteins during heat stress. Biochem. J. 329, 137–143. https://doi.org/10.1042/bj3290137.

Rudolph, A.S., Crowe, J.H., Crowe, L.M., 1986. Effects of three stabilizing agents: Proline, Betaine, and Trehalose on membrane phospholipids. Arch. Biochem. Biophys. 245, 134–143. https://doi.org/10.1016/0003-9861(86)90197-9.

Salway, J.G., 2004. Metabolism at a Glance. Wiley, Blackwell Science, London.

Schaffer, S.W., Shimada-Takaura, K., Jong, C.J., Ito, T., Takahashi, K., 2016. Impaired energy metabolism of the taurine-deficient heart. Amino Acids 48, 549–558. https://doi.org/10.1007/s00726-015-2110-2.

Schalkhausser, B., Bock, C., Stemmer, K., Brey, T., Pörtner, H.O., Lannig, G., 2013. Impact of ocean acidification on escape performance of the king scallop; *Pecten maximus*, from Norway. Mar. Biol. 160, 1995–2006. https://doi.org/10.1007/s00227-012-2057-8.

Schalkhausser, B., Bock, C., Pörtner, H.-O., Lannig, G., 2014. Escape performance of temperate king scallop, *Pecten maximus* under ocean warming and acidification. Mar. Biol. 161, 2819–2829. https://doi.org/10.1007/s00227-014-2548-x.

Schmidt, M., Windisch, H.S., Ludwichowski, K.U., Seegert, S.L.L., Pörtner, H.O., Storch, D., Bock, C., 2017. Differences in neurochemical profiles of two gadid species under ocean warming and acidification. Front. Zool. 14. https://doi.org/10.1186/s12983-017-0238-5.

Sheedy, J.R., Lachambre, S., Gardner, D.K., Day, R.W., 2016. ^{1}H-NMR metabolic profiling of abalone digestive gland in response to short-term starvation. Aquac. Int. 24, 503–521. https://doi.org/10.1007/s10499-015-9941-4.

Shumway, S.E., Koehn, R.K., 1982. Oxygen consumption in the American oyster *Crassostrea virginica*. Mar. Ecol. Prog. Ser. 9, 59–68. https://doi.org/10.3354/meps009059.

Sokolov, E.P., Sokolova, I.M., 2019. Compatible osmolytes modulate mitochondrial function in a marine osmoconformers *Crassostrea gigas* (Thunberg, 1793). Mitochondrion 45, 29–37. https://doi.org/10.1016/j.mito.2018.02.002.

Sokolova, I.M., Frederich, M., Bagwe, R., Lannig, G., Sukhotin, A.A., 2012. Energy homeostasis as an integrative tool for assessing limits of environmental stress tolerance in aquatic invertebrates. Mar. Environ. Res. 79, 1–15. https://doi.org/10.1016/j.marenvres.2012.04.003.

Somero, G.N., 2002. Thermal physiology and vertical zonation of intertidal animals: optima, limits, and costs of living. Integr. Comp. Biol. 42, 780–789. https://doi.org/10.1093/icb/42.4.780.

Somero, G.N., Yancey, P.H., 2011. Osmolytes and cell-volume regulation: physiological and evolutionary principles. In: Terjung, R. (Ed.), Comprehensive Physiology, https://doi.org/10.1002/cphy.cp140110.

Song, H., Wignall, P.B., Tong, J., Yin, H., 2013. Two pulses of extinction during the Permian–Triassic crisis. Nat. Geosci. 6, 52–56.

Stapp, L., Thomsen, J., Schade, H., Bock, C., Melzner, F., Pörtner, H.O., Lannig, G., 2017. Intra-population variability of ocean acidification impacts on the physiology of Baltic blue mussels (*Mytilus edulis*): integrating tissue and organism response. J. Comp. Physiol. B Biochem. Syst. Environ. Physiol. 187, 529–543. https://doi.org/10.1007/s00360-016-1053-6.

Stapp, L., Parker, L., O'Connor, W.A., Bock, C., Ross, P.M., Pörtner, H.O., Lannig, G., 2018. Sensitivity to ocean acidification differs between populations of the Sydney rock oyster: role of filtration and ion-regulatory capacities. Mar. Environ. Res. 135, 103–113. https://doi.org/10.1016/j.marenvres.2017.12.017.

Strobel, A., Graeve, M., Pörtner, H.O., Mark, F.C., 2013. Mitochondrial acclimation capacities to ocean warming and acidification are limited in the Antarctic Nototheniid fish, *Notothenia rossii* and *Lepidonotothen squamifrons*. PLoS One 8, e68865. https://doi.org/10.1371/journal.pone.0068865.

Sun, Y., Joachimski, M.M., Wignall, P.B., Yan, C., Chen, Y., Jiang, H., Wang, L., Lai, X., 2012. Lethally hot temperatures during the early triassic greenhouse. Science 338, 366–370.

Thompson, R.J., Livingstone, D.R., De Zwaan, A., 1980. Physiological and biochemical aspects of the valve snap and valve closure responses in the giant scallop *Placopecten magellanicus*. J. Comp. Physiol. 137, 97–104. https://doi.org/10.1007/BF00689207.

Tikunov, A.P., Johnson, C.B., Lee, H., Stoskopf, M.K., Macdonald, J.M., 2010. Metabolomic investigations of American oysters using ^{1}H-NMR spectroscopy. Mar. Drugs 8, 2578–2596. https://doi.org/10.3390/md8102578.

Tikunov, A.P., Stoskopf, M.K., Macdonald, J.M., 2014. Fluxomics of the eastern oyster for environmental stress studies. Metabolomics 4, 53–70. https://doi.org/10.3390/metabo4010053.

Tremblay, I., Guderley, H.E., 2013. Scallops show that muscle metabolic capacities reflect locomotor style and morphology. Physiol. Biochem. Zool. 87, 231–244. https://doi.org/10.1086/674107.

Tripp-Valdez, M.A., Bock, C., Lucassen, M., Lluch-Cota, S.E., Sicard, M.T., Lannig, G., Pörtner, H.O., 2017. Metabolic response and thermal tolerance of green abalone juveniles (*Haliotis fulgens*: Gastropoda) under acute hypoxia and hypercapnia. J. Exp. Mar. Biol. Ecol. 497, 11–18. https://doi.org/10.1016/j.jembe.2017.09.002.

Tripp-Valdez, M.A., Bock, C., Lannig, G., Koschnick, N., Pörtner, H.O., Lucassen, M., 2019. Assessment of muscular energy metabolism and heat shock response of the

green abalone *Haliotis fulgens* (Gastropoda: Philipi) at extreme temperatures combined with acute hypoxia and hypercapnia. Comp. Biochem. Physiol. B: Biochem. Mol. Biol. 227, 1–11. https://doi.org/10.1016/j.cbpb.2018.08.009.

Tu, C., Chen, Z.Q., Harper, D.A.T., 2016. Permian–Triassic evolution of the Bivalvia: extinction-recovery patterns linked to ecologic and taxonomic selectivity. Palaeogeogr. Palaeoclimatol. Palaeoecol. 459, 53–62. https://doi.org/10.1016/j.palaeo.2016.06.042.

Valles-Regino, R., Tate, R., Kelaher, B., Savins, D., Dowell, A., Benkendorff, K., 2015. Ocean warming and CO_2- induced acidification impact the lipid content of a marine predatory gastropod. Mar. Drugs. 13, 6019–6037. https://doi.org/10.3390/md13106019.

Venter, L., Loots, D.T., Mienie, L.J., Jansen van Rensburg, P.J., Mason, S., Vosloo, A., Lindeque, J.Z., 2018. The cross-tissue metabolic response of abalone (*Haliotis midae*) to functional hypoxia. Biol. Open 7. https://doi.org/10.1242/bio.031070.

Viant, M.R., Rosenblum, E.S., Tjeerdema, S., 2003. NMR-based metabolomics: a powerful approach for characterizing the effects of environmental stressors on organism health. Environ. Sci. Technol. 37, 4982–4989. https://doi.org/10.1021/es034281x.

Wang, W., Wu, Z., Dai, Z., Yang, Y., Wang, J., Wu, G., 2013. Glycine metabolism in animals and humans: implications for nutrition and health. Amino Acids 45, 463–477. https://doi.org/10.1007/s00726-013-1493-1.

Weidlich, O., Kiessling, W., Flügel, E., 2003. Permian-Triassic boundary interval as a model for forcing marine ecosystem collapse by long-term atmospheric oxygen drop. Geol. 31, 961–964.

Wignall, P.B., Twitchett, R.J., 1996. Oceanic anoxia and the end Permian mass extinction. Science 272, 1155–1158. https://doi.org/10.1126/science.272.5265.1155.

Wilkens, L.A., 2006. Neurobiology and behavior of the scallop. In: Shumway, S.E., Parson, G.J. (Eds.), Scallops: Biology, Ecology and Aquaculture, 1st edn. Elsevier, Amsterdam, pp. 317–356.

Wittmann, A.C., Pörtner, H.O., 2013. Sensitivities of extant animal taxa to ocean acidification. Nat. Clim. Chang. 3, 995–1001. https://doi.org/10.1038/nclimate1982.

Xia, J., Wishart, D.S., 2010. MetPA: a web based metabolomics tool for pathway analysis and visualization. Syst. Biol. 26, 2342–2344. https://doi.org/10.1093/bioinformatics/btq418.

Xia, J., Wishart, D.S., 2016. Using MetaboAnalyst 3.0 for comprehensive metabolomics data analysis. Curr. Protoc. Bioinformatics 55, 14.10.1–14.10.91. https://doi.org/10.1002/cpbi.11.

Yancey, P.H., 2005. Organic osmolytes as compatible, metabolic, and counteracting cytoprotectants in high osmolarity and other stresses. J. Exp. Biol. 208, 2819–2830. https://doi.org/10.1242/jeb.01730.

Zittier, Z., Bock, C., Lannig, G., Pörtner, H.O., 2015. Impact of ocean acidification on thermal tolerance and acid–base regulation of *Mytilus edulis* (L.) from the North Sea. J. Exp. Mar. Biol. Ecol. 473, 16–25. https://doi.org/10.1016/j.jembe.2015.08.001.

Zittier, Z., Bock, C., Sukhotin, A.A., Häfker, N.S., Pörtner, H.O., 2018. Impact of ocean acidification on thermal tolerance and acid–base regulation of Mytilus edulis from the White Sea. Polar Biol. 41, 2261–2273.